

index change.

Another powerful diagnostic tool for photonic lattices is offered by the recently demonstrated Brillouin zone spectroscopy [12]. The aim of this method is a direct visualization of the lattice structure in Fourier space by mapping the boundaries of the extended Brillouin zones, which are defined through the Bragg-reflection planes. To map out the momentum space, the lattice is probed with a partially spatially incoherent beam, which has a uniform spatial power spectrum extending over several Brillouin zones and is broad enough in real space to cover numerous lattice sites. The light exiting the lattice is then analysed by performing an optical Fourier transformation and measuring the power spectrum, which contains dark lines at the borders of the extended Brillouin zones.

In this contribution we apply both methods to analyze the induced refractive index change of two-dimensional photonic lattices in a photorefractive crystal. For the first time to our knowledge, a Fourier space analysis of two-dimensional nonlinear self-trapped photonic lattices with periodic phase modulation is performed by mapping the borders of the extended Brillouin zones. We compare the results obtained in Fourier space and in real space and demonstrate that both methods are able to show the differences between linear and nonlinear lattices. We also show that both methods reveal the orientational dependent structure of the nonlinear induced refractive index change.

II. EXPERIMENTAL ARRANGEMENTS

The experimental setup is shown schematically in Fig. 1. A beam derived from a frequency doubled Nd:YAG laser at a wavelength of 532 nm is split into two beams by a combination of a half wave plate and a polarizing beam splitter. The transmitted beam is sent through a combination of two quarter wave plates and a programmable spatial light modulator in order to induce the desired pure phase modulation onto the beam. The modulated beam is then imaged by a high numerical aperture telescope at the input face of a 20 mm long $\text{Sr}_{0.60}\text{Ba}_{0.40}\text{Nb}_2\text{O}_6$ (SBN:Ce) crystal, which is biased by an externally applied electric field and uniformly illuminated with a white-light source to control the dark irradiance. The polarization can be adjusted using a half wave plate in front of the telescope so that linear and nonlinear lattices can be induced. By switching off the modulator, the lattice can be illuminated with a broad plane wave to observe the waveguiding properties. The second beam is passed through a rotating diffuser and the partially spatially incoherent output of the diffuser is imaged at the front face of the crystal. To ensure that the light will experience the refractive index modulation of the lattice, the beam is extraordinarily polarized using a half wave plate. The output of the crystal is analysed with two CCD cameras. CCD1 monitors the real space

output, whereas CCD2 is placed in the focal plane of a lens to visualize the Fourier power spectrum of the light exiting the lattice.

In the following experiments, the lattice period is about $22 \mu\text{m}$ and the applied electric field is 1 kV/cm .

III. SQUARE PATTERN

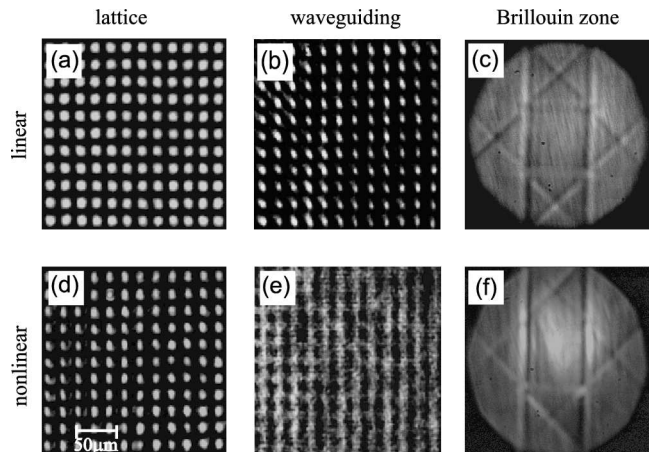


FIG. 2: Experimentally generated light intensity patterns for linear and nonlinear square lattices: (a)/(d) lattice output, (b)/(e) guided wave, (c)/(f) Brillouin zone

Fig. 2(a) depicts the output intensity distribution for the linear, i.e. ordinarily polarized square lattice at the back face of the crystal. Compared to the nonlinear, i.e. extraordinarily polarized lattice output [Fig. 2(d)], the only difference is a self focussing of each spot in the nonlinear case. The difference between linear and nonlinear square lattices becomes more obvious by observing the waveguiding properties of the induced lattice [Fig. 2(b) and (e)]. The linear wave induces a truly two-dimensional array of effective focusing lenses and the output intensity distribution of the guided wave shows a simple square pattern, too [Fig. 2(b)]. In contrast to that, the lattice spots in the nonlinear case tend to fuse into vertical lines due to nonlocality and anisotropy of the photorefractive response. Therefore, the output intensity distribution of the guided wave reveals an effectively one-dimensional refractive index change that basically consists of vertical lines [Fig. 2(e)]. This is in good agreement with previously performed numerical simulations [9, 11]. The Fourier space analysis of the induced refractive index change confirms this difference between linear and nonlinear lattices. The Brillouin zone of the linear induced lattice reveals a fully two-dimensional structure and clearly shows the corresponding first and second Brillouin zone [Fig. 2(c)]. The slightly different contrast for horizontal and vertical lines is due to the anisotropy of the photorefractive material. On the other hand, the Brillouin zone picture of the nonlinear lattice is dominated by two vertical lines representing the borders of the

first Brillouin zone of the corresponding one-dimensional stripe pattern [Fig. 2(f)]. Additional lines from the originally two-dimensional lattice are also visible, but the two vertical lines are obviously more intense.

IV. DIAMOND PATTERN

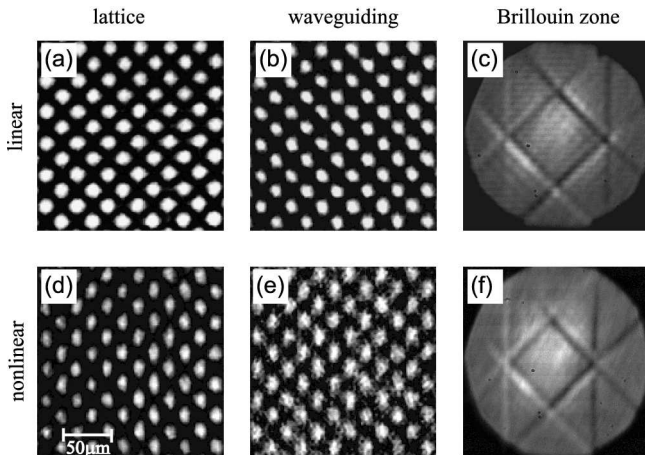


FIG. 3: Experimentally generated light intensity patterns for linear and nonlinear diamond lattices: (a)/(d) lattice output, (b)/(e) guided wave, (c)/(f) Brillouin zone

Fig. 3 shows the results obtained for the diamond pattern. Comparing the output intensity distributions of the lattice waves, the only difference is again found in a self focussing of the single spots for the nonlinear lattice [Fig. 3(d)]. As before, the intensity distribution of the guided wave in the linear lattice basically follows the intensity distribution of the lattice output. However, the waveguiding of the nonlinear induced lattice also shows a fully two-dimensional structure consisting of well separated spots that do not fuse into vertical lines, as seen for the square pattern [Fig. 3(e)]. This orientational dependent structure of the nonlinear induced refractive index change fits well to our numerical simulations, too [9, 11].

As the waveguiding method does not show any significant difference between the induced refractive index structure for linear and nonlinear lattices, the Fourier space analysis should consequently result in two similar Brillouin zone pictures. This is shown in Fig. 3(c) and (f). In contrast to the square pattern, the Brillouin zone picture of both, the linear and the nonlinear diamond pattern clearly reveals a fully two-dimensional structure of the induced refractive index change.

V. CONCLUSIONS

We have generated experimentally linear and nonlinear two-dimensional self-trapped photonic lattices with different orientations in an anisotropic photorefractive medium. The differences of the induced refractive index change depending on polarization and spatial orientation of the periodic lattice wave have been investigated with two different approaches. For the first time to our knowledge, partially spatially multi-band excitation has been used to analyze the structure of two-dimensional nonlinear self-trapped photonic lattices in Fourier space. Furthermore the waveguiding properties of the lattice have been observed to achieve a real space analysis of the induced refractive index change. Both methods clearly reveal the discussed structural differences of the induced refractive index change and therefore provide powerful diagnostic tools for further experiments on nonlinear photonic lattices.

Acknowledgments

We thank Guy Bartal and Mordechai Segev, Solid State Institute, Technion, Haifa for fruitful discussions on the Brillouin zone spectroscopy. We are also grateful to Zhigang Chen, Department of Physics and Astronomy, San Francisco State University for critical reading of the manuscript. DT acknowledges support by the Konrad-Adenauer-Stiftung e.V.

-
- [1] Y.S. Kivshar and G.P. Agrawal, *Optical Solitons: From Fibers to Photonic Crystals* (Academic, San Diego, 1993).
 - [2] J. W. Fleischer, M. Segev, N. K. Efremidis, and D. N. Christodoulides, *Nature* **422**, 147 (2003)
 - [3] Z. Chen and K. McCarthy, *Opt. Lett.* **27**, 2019 (2002)
 - [4] S. Minardi, S. Sapone, W. Chinaglia, P. Di Trapani, and A. Berzanskis, *Opt. Lett.* **25**, 326 (2000)
 - [5] J. Petter, J. Schröder, D. Träger, and C. Denz, *Opt. Lett.* **28**, 438 (2003)
 - [6] D. Neshev, Y. S. Kivshar, H. Martin, and Z. G. Chen, *Opt. Lett.* **29**, 486 (2004)
 - [7] H. Martin, E. D. Eugenieva, Z. Chen, and D. N. Christodoulides, *Phys. Rev. Lett.* **92**, 123902 (2004)
 - [8] M. Petrovic, D. Träger, A. Strinic, M. Belic, J. Schröder, and C. Denz, *Phys. Rev. E* **68**, 055601R (2003)
 - [9] A. S. Desyatnikov, D. N. Neshev, Y. S. Kivshar, N. Sagemerten, D. Träger, J. Jägers, C. Denz, and Y. V. Kartashov, *Opt. Lett.* **30**, 869 (2005)
 - [10] D. Träger, A. Strinic, J. Schröder, C. Denz, M. Belic, M. Petrovic, S. Matern, and H. G. Purwins, *J. Opt. A Pure Appl. Opt.* **5**, 518-523 (2003)
 - [11] A. S. Desyatnikov, N. Sagemerten, R. Fischer, B. Terhalle, D. Träger, D. N. Neshev, A. Dreischuh, C. Denz, W. Krolikowski, and Y. S. Kivshar, *Opt. Expr.* **14**, 2851-2863 (2006)
 - [12] G. Bartal, O. Cohen, H. Buljan, J. W. Fleischer, O.

Manela, and M. Segev, Phys. Rev. Lett. **94**, 163902-4
(2005)